International Journal of Nanoelectronics and Materials
Volume 15 (Special Issue) December 2022 [119-129]

Physical and Optical Characteristics of α-Al_2O_3 Nano Coating formed by Pulsed Laser Deposition Technique

Ayman M. Hassan[1], Ali A. Alwahib[2*], and Abbas K. Hussein[3]

[1]Laser and Optoelectronics Department, University of Technology-Iraq, Baghdad, Iraq
[2]Laser and Optoelectronics Department, University of Technology-Iraq, Baghdad, Iraq
[3]Nanotechnology and Advanced Materials Research Center, University of Technology-Iraq, Baghdad, Iraq

ABSTRACT

Due to the importance of Al_2O_3 nano-coatings in different fields, further studies and investigations are required. In addition, few studies about preparing Al_2O_3 by pulsed laser deposition have been found; hence this method was selected for Al_2O_3 preparation. Alumina (α-Al_2O_3) is deposited to form nano-coating film using pulsed laser deposition (PLD) on Indium Tin Oxide (ITO) substrate. Laser pulses are applied in three sets of 100, 200, and 300. The combination of the number of laser pulses and energies of 700, 800, and 900 mJ are made to study the crystal structure, surface morphology, and optical properties of the nano-coated. The crystal structure analyses using XRD showed that nano-coating has a polycrystalline structure. The AFM analyses showed that the average surface roughness proportion with the energy and the number of pulses increased from 0.6 nm to 2.9 nm. The transmission decreased with increasing laser energy and the number of pulses. The optical bandgap from 4.11 to 4.01ev is also obtained. For the first time, this study demonstrates three energies and three sets of pulses associated with a fixed substrate temperature of 200ºC; optical characteristics were studied extensively under PLD technique conditions.

Keywords: Number of pulses, energy, PLD, nano-coating

1. INTRODUCTION

Nanocoating is a thin layer ranging from 1nm to several hundreds of nanometers in thickness [1]. Nanocoating is used in many applications such as solar cells [2], microelectronics[3], and several applications. The study of the physical properties of nano-coating is critical to applying it in any field.

Alumina (Al_2O_3) nano-coating is one of the most prominent types of oxide nano-coating due to its good physical properties [4]. Al_2O_3 nano-coating is used in passivating solar cells [5], anti-reflective coatings [6], and transparent electronic devices[7]. There are several methods for preparing Al_2O_3 nano-coating, such as atomic layer deposition[8], plasma-enhanced chemical vapor deposition [9], and pulsed laser deposition(PLD) [10].

Alumina has different phases; the gamma phase (γ-Al_2O_3) and alpha phase (α-Al_2O_3) are the most prominent [11]. The α-Al_2O_3 is characterized by a high melting point, high hardness, and chemical stability, which allows it to be used as a coating layer [12]. In contrast, the γ-Al_2O_3 is chemically unstable and used as an intermediate in chemical reactions[13]. The α-Al_2O_3 crystal lattice is characterized by its Hexagonal shape [14], while the γ-Al_2O_3 phase has two types of crystal lattices, either octagonal [15] or tetrahedral [16]. Both phases can be deposited as thin layers using different methods, such as evaporation and laser light interaction.

*Ali.A.Alwahib@uotechnology.edu.iq

Pulsed laser deposition is a physical vapor deposition (PVD) method applied in thin-film preparation [17]. Unique properties of PLD technology can be gained to prepare coatings from any material [18]. The deposition process can be managed by the laser and vacuum chamber parameters. Laser parameters are the wavelength (λ), the number of pulses, pulse energy (E), pulse width (W), spot size (S), and pulse repetition rate (Rr). Moreover, the vacuum chamber parameters are the distance between the substrate and the target (d), the substrate temperature (T), and the pressure of the vacuum chamber (P).

In this research work, α-Al_2O_3 was deposited using the PLD method supported by hundreds of pulses based on energies. The physical relationship between three pluses and three laser energies proves recognizable effects on the optical characteristics of the generating thin film. The results are supported by AFM test and XRD test to study the variations according to the power value.

2. EXPERIMENTAL WORK

A mechanical pressing device was used to prepare a solid target from α-Al_2O_3 powder (99.9% purity). Sixteen tons of weight was applied to press 4g of α-Al_2O_3 powder in 7 minutes. A circular α-Al_2O_3 target with a thickness of 0.5 cm and a diameter of 2 cm was obtained. α-Al_2O_3 was deposited on a substrate by using Nd: YAG laser (λ=1064nm) with a repetition rate of 3Hz, a pulse width of 7ns, and a spot size of 0.8nm. The substrate was placed at a three centimeters distance from the target; the pressure of the vacuum chamber was 10^{-3} mbar; the angle between the target and the laser source line was 45º (Figure 1). Three Different energies (700, 800, 900 mJ) and 100, 200, and 300 pulses at 200ºC substrate temperature were applied to deposit α-Al_2O_3 on the Indium Tin Oxide (ITO). ITO substrate has good hardness, high transmittance, and can withstand high temperatures, making it suitable for the PLD deposition method [18].

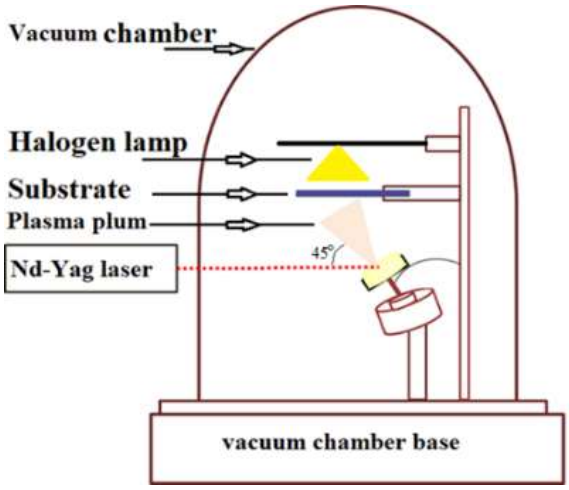

Figure 1. Pulsed Laser Deposition (PLD) technique.

The structural analyses of the α-Al_2O_3 nano-coating were carried out using the X-ray diffraction technique (Shimadzu XRD.6000) equipped with a Cu-ka radiation system at a wavelength (0.154nm) of 30 mA and 40 kilovolts. The scanning angle ranged from 20° to 80°. Atomic force microscopy (TT-2AFM) investigated the material's morphology. The spectroscopic analyses of the α-Al_2O_3 nano-coating were carried out using a UV-VIS SP8001 and performed from 200 to 1000 nm for the prepared nano-coating. The average roughness (Ra), root mean square (RMS), transmittance, and energy gap were studied.

Measuring the thickness of the nano-coating on the substrate is critical because the physical properties of the nano-coating largely depend on the thickness. Fizeau interferometer non-destructive method was used to measure the thickness. After using the Fizeau interferometry technique, the Fizeau fringes appeared, as shown in Figure 2.

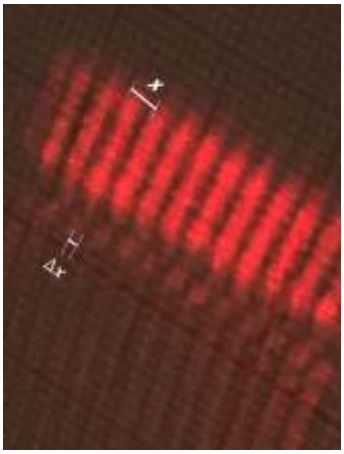

Figure 2. The Fizeau fringes of α-Al_2O_3 nano-coating.

The thickness of the coating was calculated using the following mathematical formula [19]:

$$t = \frac{\lambda \Delta x}{2x} \quad (1)$$

T : the thickness of the coating(nm), $\lambda = 632.8nm$, x: the shift between interference fringes
Δx : fringe width

3. RESULTS AND DISCUSSION

The thickness of the nano-coating is critical because the physical properties largely depend on the thickness. The thickness was measured according to the number of depositing pulses, as shown in Figure 3. The thickness values vary in proportion to the number of pulses, and these values increase by increasing the applied power.

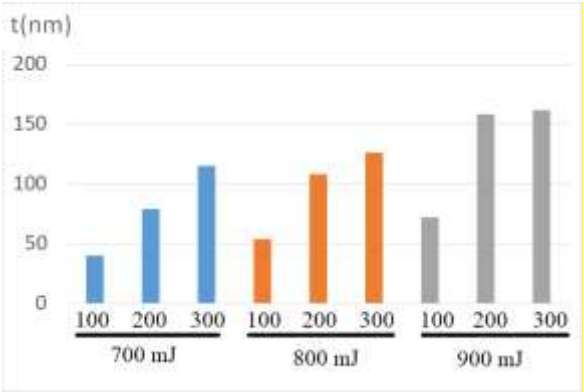

Figure 3. Thickness varies according to the number of pulses and energy values

The target absorbance depends on the intensity, wavelength of the laser light, and the target material's electronic composition [19]. When the photon is combined with the material's electron, it leads to a local increase in temperature and, thus a thermal mechanism. This thermal mechanism leads to the evaporation of the material from the surface of the target. The vaporized material is the plasma plume that contains nanoparticles, ions, and atoms [20]. The laser energy and the number of pulses determine the amount of material removed from the target surface. As the energy increases, the density of the generated plasma and coatings thickness increase, as shown in Figure 4.

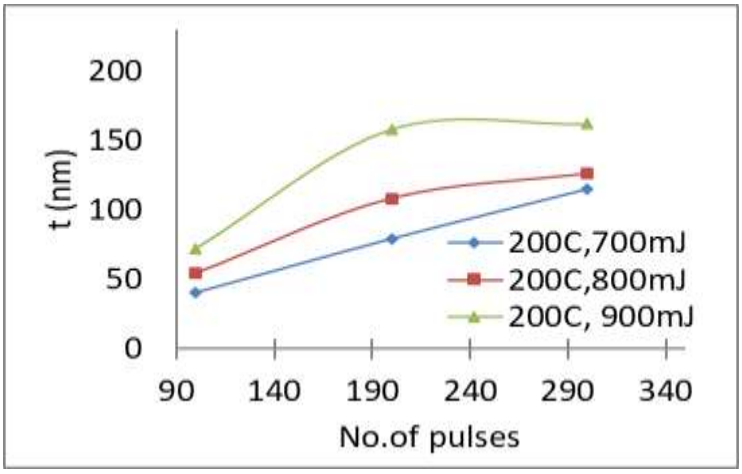

Figure 4. Relationship between coating thickness and number of pulses

XRD analyses of the coating layer (alumina) show a polycrystalline structure due to the different peaks at diffraction patterns (104), (110), (024), and (211) that have appeared, as shown in Figure 5. The results are identical to the card number (96-100-0018) used in the Match!3 programs. The results are also compatible with the results of Lauri A. et al.[12]and Ram P. et al. [21]. It was noticed in Figure 4 that the intensity of the diffraction plane 104 is higher than the other peaks; This can be explained by the presence of more periodicity in the direction of the crystals [22]. In Table 1, the predominant plane (104) showed a slight shifting due to the laser energy, and the number of pulses increased. The change in the diffraction Peak Position (2θ) is a change in the distance between the levels (d-spacing) that occurs by the change in the lattice constants. The variable in d-spacing is the variable in the thickness of the nano-coating [23].

The crystallite size (D) was calculated as shown in Table (3) by using the Scherrer's formula [24]:

$$D = \frac{k\lambda}{\beta\, Cos\theta} \qquad (2)$$

Where k: Scherer constant = 0.9 λ: 0.154nm β: Full width at half maximum (FWHM) (rad.)

In Table 1, the peak (104) crystallite size increased with the increased energy and number of laser pulses because the density of the plasma's kinetic energy increased [25]. This event leads to the mobility of deposited atoms on the substrate surface can be enhanced by the higher laser incident energy [25]. It can also be noticed that full width at half maxima is inversely proportional to the crystallites' size. Since laser energy caused the larger size of crystallites thus, the FWHM of the predominant peaks was decreased. This event leads to the mobility of deposited atoms on the substrate surface can be enhanced by the higher laser incident energy [25]. The crystallite size of the predominant plane (104) increased from 15.191 nm to 23.869 nm for coatings deposited at 700 mJ (100 pulses) to 900 mJ (300 pulses), respectively.

Table 1 XRD Structural parameters of α-Al_2O_3 nano-coating with variable energies deposition and pulse laser at substrate temperature 200ºC

E (mJ)	No. of pulse	2θ (deg.)	FWHM (deg.)	d (A)	D (nm)	hkl
700	100	35.3983	0.5487	2.53372	15.1918352	104
		37.6339	0.2967	2.38819	28.27632571	110
		50.9638	0.482	1.76327	18.2509369	024
		60.974	0.64	1.5183	14.39883887	211
	200	35.3932	0.42	2.53408	19.84676569	104
		37.5456	0.3	2.38747	27.95795335	110
		50.7739	0.412	1.7967	21.33500322	024
		60.3942	0.58	1.53148	15.84138777	211
	300	35.3782	0.3585	2.53512	23.25047008	104
		37.5623	0.4933	2.39258	17.00344939	110
		50.7412	0.4667	1.79779	18.83186523	024
		60.3862	0.28	1.53167	32.81297022	211
800	100	35.3825	0.3781	2.53482	22.04547285	104
		37.9554	0.32	2.3687	26.24264791	110
		50.7979	0.54	1.79591	16.27943566	024
		60.3442	0.5733	1.53263	16.0224548	211
	200	35.3766	0.371	2.5354	22.4669984	104
		37.4845	0.32	2.3971	26.20583563	110
		50.7472	0.4	1.7976	21.97262436	024
		60.3762	0.442	1.5319	20.78544164	211
	300	35.3814	0.3551	2.5349	23.473297	104
		37.6422	0.3061	2.38768	27.40866688	110
		50.8558	0.4377	1.794	20.08911562	024
		60.1843	0.384	1.53632	23.90165792	211
900	100	35.3721	0.4412	2.5355	18.89200368	104
		37.4887	0.36	2.3998	23.29436582	110
		50.5762	0.53	1.8013	16.57140305	024
		60.7753	0.36	1.5228	25.57186879	211
	200	35.3701	0.3938	2.53568	21.16583453	104
		37.499	0.3267	2.39647	25.66950574	110
		50.6612	0.4933	1.80044	17.81051083	024
		60.1043	0.24	1.53818	38.2271966	211
	300	35.395	0.3493	2.53395	23.86396613	104
		37.6956	0.36	2.38442	23.30868506	110
		50.508	0.36	1.80554	24.38993422	024
		60.4275	0.263	1.53072	34.94129035	211

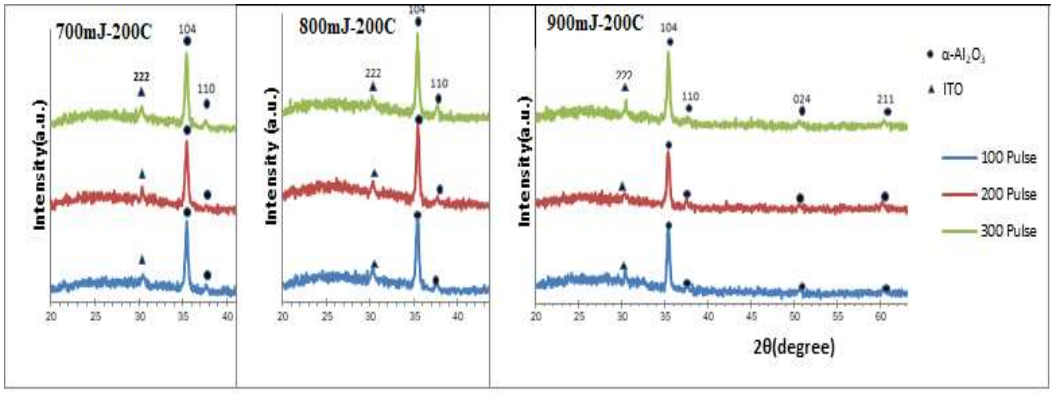

Figure 5. The XRD spectrum of α-Al2O3 nano-coating at different energy and number of laser pulses at substrate temperature 200°C.

In Table 2, the root means square (RMS) and the average surface roughness (Ra) were found. The surface roughness increased with increasing the energy and the number of laser pulses due to the increase in the particle size [26]. At 700 mJ and 100 laser shots, the Ra =0.6 and RMS=0.91 nm were the lowest among other conditions, as compared with the highest surface roughness values (Ra=2.9 and RMS roughness =4.6 nm) that resulted from increasing the laser energy and the number of pulses to 900 mJ and 300 pulses.

Table 2 RMS and Ra of α-Al_2O_3 at different conditions

E (mJ)	No. pulse	t (nm)	Ra	Rms
700	100	40	0.6	0.91
700	200	79	1.35	2.02
700	300	115	2.35	3.89
800	100	54	1.12	1.81
800	200	108	1.84	3.02
800	300	126	2.58	4.15
900	100	72	1.28	1.83
900	200	158	2.25	3.5
900	300	162	2.9	4.6

The surface morphologies of the samples, deposited at different energies and numbers of pulses, were investigated by AFM. The three-dimensional and two-dimensional morphological images of the α-Al_2O_3 coating are shown in Figure 6. The images of coatings show that the particle distribution on the surface is not homogeneous with different energies and numbers of pulses. The particle size was increased with increasing energy and the number of laser pulses; this is because the large particles appear due to the high thermal stress resulting from the interaction of the high energy of the laser pulse with the target material [27].

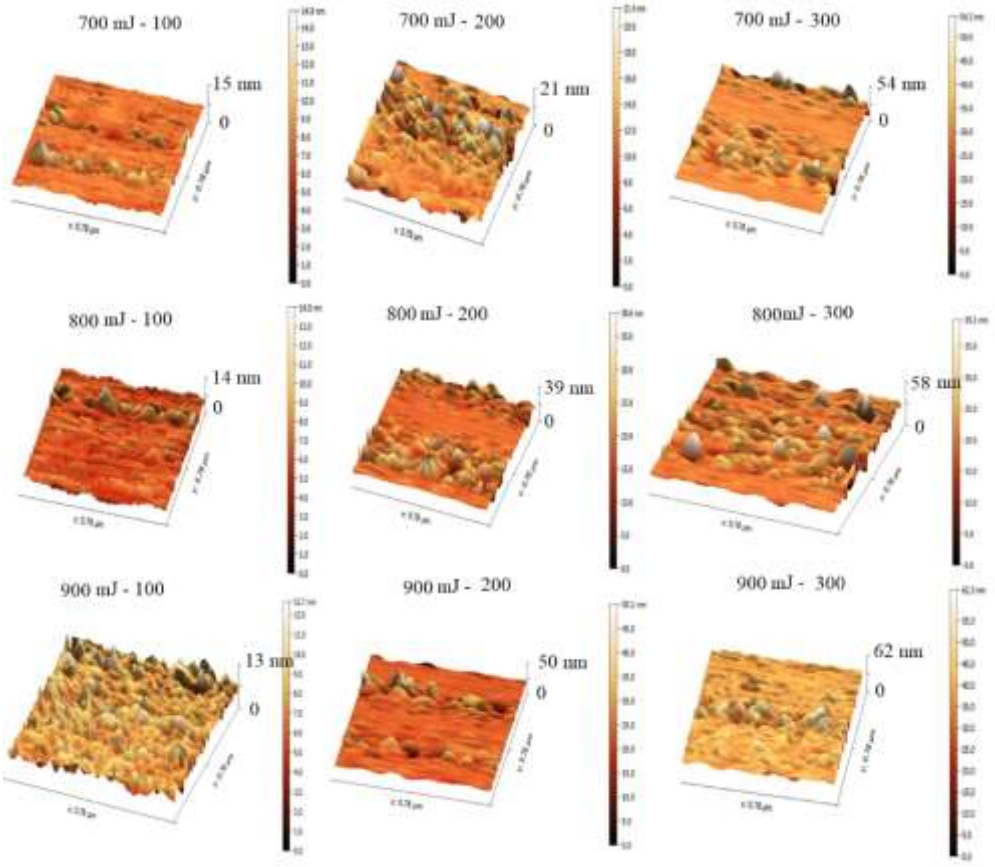

Figure 6. 3D AFM images of the α-Al_2O_3 layer at different conditions.

Figure 6 shows the optical transmission spectra of the α-Al_2O_3 layer in the wavelength range from 200 to 1000 nm. All Coatings have maximum transmission at the visible region and a sharp absorption range between 200 to 300 nm. The transmittance decreased with the increase in the deposition energy and the number of pulses due to the surface roughness, coating thickness, size, and defects of the formed particles. With increasing the thickness, the micro defect defects will accumulate and cause reduces in transmittance [28]. The disadvantages of the coating are the particle size and distribution, which all affect the transmission of the coating. It is noted in this work that the surface roughness is relatively low, so no effect on the permeability is expected. The high roughness increases the scattering of light, thus reducing the transmittance [29]. It is noted that the surface roughness is relatively low, so it does not significantly affect the transmission of the coating.

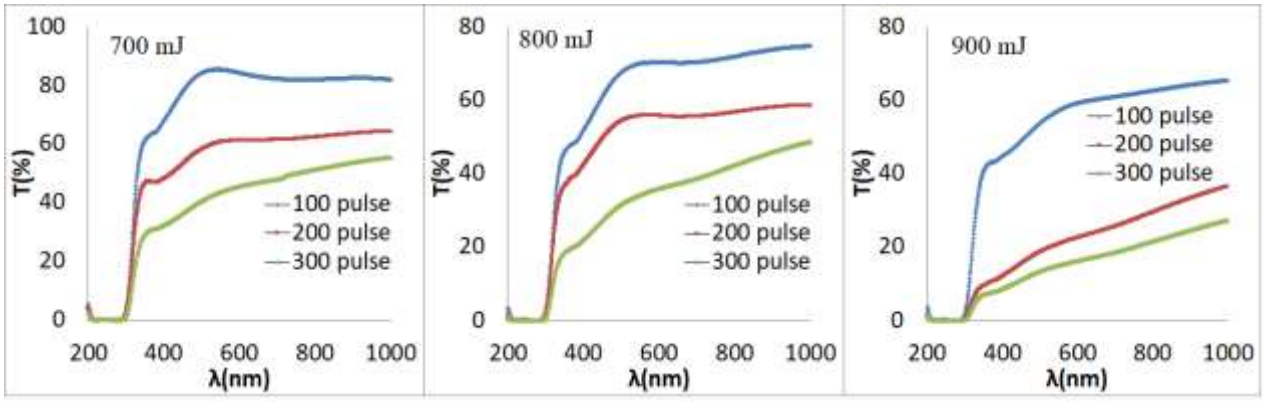

Figure 7. Optical transmittance at different irradiate energy.

In Table 3, the optical bandgap energy decreased for all energies by increasing the number of laser pulses. Usually, increasing the number of pulses leads to an increased thickness layer of the deposited material. The crystal's size and coating density are the main features related to the coating thickness [29]; variation of these features is the main reason for reducing the bandgap energy. In addition, increasing the laser energy caused a higher photon-electron coupling that induced a higher absorption of the material target, thus a higher ejection. This behavior is the main reason for reducing the bandgap energy [30].

Table 3 Optical band gap of α-Al_2O_3 nano- coating

E (mJ)	No. Pulse	Eg (eV)
700	100	4.11
700	200	4.10
700	300	4.08
800	100	4.10
800	200	4.09
800	300	4.07
900	100	4.09
900	200	4.06
900	300	4.01

The optical bandgap of the α-Al_2O_3 coating can be determined by the following Equation.[31]

$$\alpha = \frac{(h\nu - E_g)^2}{h\nu} \quad (3)$$

Where hν and Eg are photon energy and band gap values, respectively. The absorption coefficient α was obtained from the transmittance data using the relation a = (1/t) ln(1/T)[32], where T and d are the transmittance and the thickness of the obtained coatings, respectively.

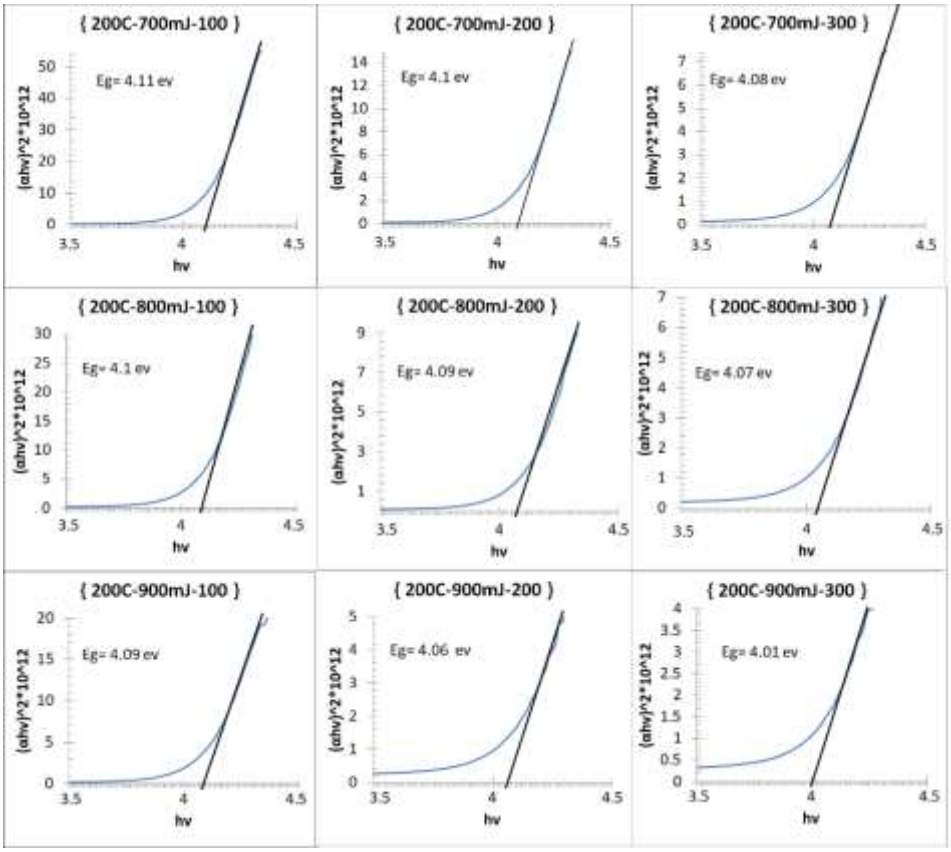

Figure 8. The optical band gap of α-Al_2O_3 nano-coating

4. CONCLUSION

A systematic study was carried out on the effect of laser energy and the number of pulses on the growth of α-Al_2O_3 nano-coating. α-Al_2O_3 nano-coating was obtained by depositing α-Al_2O_3 powder on ITO substrates by using PLD technique. Different laser energy and pulses were used at a constant substrate temperature to prepare the α-Al2O3 nano-coating. The properties of the deposited samples were studied using XRD, AFM, and UV-VIS techniques. XRD analysis showed that all nano-coating is polycrystalline, and the size of the crystals changes with the change in the energy and laser pulses. AFM analysis was used to study the surface nature of nano-coating. The analysis results showed that the average roughness and root mean square increased with the increasing laser energy and pulses. An increase in laser energy and pulses led to high plasma plums containing large particle sizes produced from the target. Large particle size produced large surface roughness. UV-VIS analysis showed the sharp absorbance of all nano-coating in the ultraviolet (UV) region. The high transmission was shown in the spectrum region. The transmission and optical band gap were decreased with increased energy and laser pulses.

ACKNOWLEDGEMENTS

The author is grateful to the University of Technology-Iraq for a great support.

REFERENCES

[1] V. Grumezescu and I. Negut, Nanocoatings and thin films. Elsevier Inc., 2019.

[2] M. S. Mozumder, A. H. I. Mourad, H. Pervez, and R. Surkatti. Recent developments in multifunctional coatings for solar panel applications: A review, Sol. Energy Mater. Sol. Cells, vol. 189, no. June 2018, pp. 75–102, 2019, doi: 10.1016/j.solmat.2018.09.015.

[3] J. Sudagar, J. Lian, and W. Sha. Electroless nickel, alloy, composite and nano coatings - A critical review, J. Alloys Compd., vol. 571, pp. 183–204, 2013, doi: 10.1016/j.jallcom.2013.03.107.

[4] D. A. Mohammed, A. Kadhim, and M. A. Fakhri. The enhancement of the corrosion protection of 304 stainless steel using Al2O3 films by PLD method, AIP Conf. Proc., vol. 2045, no. December 2018, pp. 0–6, 2018, doi: 10.1063/1.5080827.

[5] J. Benick, A. Richter, M. Hermle, and S. W. Glunz. Thermal stability of the Al2O3 passivation on p-type silicon surfaces for solar cell applications," Phys. Status Solidi - Rapid Res. Lett., vol. 3, no. 7–8, pp. 233–235, 2009, doi: 10.1002/pssr.200903209.

[6] C. Yin et al. Al 2 O 3 anti-reflection coatings with graded-refractive index profile for laser applications, Opt. Mater. Express, vol. 11, no. 3, p. 875, 2021, doi: 10.1364/ome.418174.

[7] D. A. Mohammed, A. Kadhim, and M. A. Fakhri. The enhancement of the corrosion protection of 304 stainless steel using Al2O3 films by PLD method, AIP Conf. Proc., vol. 2045, no. December, 2018, doi: 10.1063/1.5080827.

[8] R. Zazpe et al. Atomic Layer Deposition Al2O3 Coatings Significantly Improve Thermal, Chemical, and Mechanical Stability of Anodic TiO2 Nanotube Layers, Langmuir, vol. 33, no. 13, pp. 3208–3216, 2017, doi: 10.1021/acs.langmuir.7b00187.

[9] W. Ban, S. Kwon, J. Nam, J. Yang, S. Jang, and D. Jung, "Al2O3 thin films prepared by plasma-enhanced chemical vapor deposition of dimethylaluminum isopropoxide," Thin Solid Films, vol. 641, pp. 47–52, 2017, doi: 10.1016/j.tsf.2017.02.007.

[10] M. A. Fakhri, S. F. H. Alhasan, N. H. Numan, J. M. Taha, and F. G. Khalid, Effects of laser wavelength on some of physical properties of Al2O3 nano films for optoelectronic device, AIP Conf. Proc., vol. 2213, no. March, 2020, doi: 10.1063/5.0000183.

[11] G. Balakrishnan et al., Structural and optical properties of γ-alumina thin films prepared by pulsed laser deposition, Thin Solid Films, vol. 518, no. 14, pp. 3898–3902, 2010, doi: 10.1016/j.tsf.2009.12.001.

[12] L. Aarik, H. Mändar, P. Ritslaid, A. Tarre, J. Kozlova, and J. Aarik, Low-Temperature Atomic Layer Deposition of α-Al2O3Thin Films, Cryst. Growth Des., vol. 21, no. 7, pp. 4220–4229, 2021, doi: 10.1021/acs.cgd.1c00471.

[13] Y. Rozita, R. Brydson, and A. J. Scott, An investigation of commercial gamma-Al 2 O 3 nanoparticles, J. Phys. Conf. Ser., vol. 241, p. 012096, 2010, doi: 10.1088/1742-6596/241/1/012096.

[14] D. P. Sigumonrong, D. Music, and J. M. Schneider, Efficient supercell design for surface and interface calculations of hexagonal phases: α-Al2O3 case study, Comput. Mater. Sci., vol. 50, no. 3, pp. 1197–1201, 2011, doi: 10.1016/j.commatsci.2010.11.020.

[15] A. Akbarzadeh, M. Ahmadlouydarab, and A. Niaei, Capabilities of α-Al2O3, γ-Al2O3, and bentonite dry powders used in flat plate solar collector for thermal energy storage, Renew. Energy, vol. 173, pp. 704–720, 2021, doi: 10.1016/j.renene.2021.04.026.

[16] B. Ealet, M. H. Elyakhloufi, E. Gillet, and M. Ricci, Electronic and crystallographic structure of γ-alumina thin films, Thin Solid Films, vol. 250, no. 1–2, pp. 92–100, 1994, doi: 10.1016/0040-6090(94)90171-6.

[17] I. Najm, A. Alwahib, and S. Kadhim, Study of CuS Thin Films Deposited by PLD Simulated for Prism Based SPR Sensor, Eng. Technol. J., vol. 39, no. 6, pp. 936–945, 2021, doi: 10.30684/etj.v39i6.1973.

[18] Z. Ghorannevis, E. Akbarnejad, and M. Ghoranneviss, Structural and morphological properties of ITO thin films grown by magnetron sputtering, J. Theor. Appl. Phys., vol. 9, no. 4, pp. 285–290, 2015, doi: 10.1007/s40094-015-0187-3.

[19] I. L. Quintás, Characterization and control of laser ablation plasmas for the synthesis of new materials and as optical nonlinear media, 2017.
[20] H. Yu, H. Li, Y. Wang, L. Cui, S. Liu, and J. Yang, Brief review on pulse laser propulsion, Opt. Laser Technol., vol. 100, pp. 57–74, 2018, doi: 10.1016/j.optlastec.2017.09.052.
[21] R. Prakash, S. Kumar, V. Kumar, R. J. Choudhary, and D. M. Phase, Optical and x-ray photoelectron spectroscopy studies of α-Al2O3, AIP Conf. Proc., vol. 1731, pp. 10–13, 2016, doi: 10.1063/1.4947751.
[22] C. Outline, Methods for Assessing Surface Cleanliness, vol. 12. 2019.
[23] T. Atwee, A. S. Gadallah, M. A. Salim, and A. M. Ghander, "Effect of film thickness on structural, morphological, and optical properties of Cu2ZnSnS4 thin films prepared by sol–gel spin coating, Appl. Phys. A Mater. Sci. Process., vol. 125, no. 4, pp. 1–10, 2019, doi: 10.1007/s00339-019-2570-4.
[24] C. Wang et al., Structural, optical and morphological evolution of Ga2O3/Al2O3 (0001) films grown at various temperatures by pulsed laser deposition, Ceram. Int., vol. 47, no. 21, pp. 29748–29757, 2021, doi: 10.1016/j.ceramint.2021.07.147.
[25] S. M. Pawar et al., Effect of laser incident energy on the structural, morphological and optical properties of Cu2ZnSnS4 (CZTS) thin films, Curr. Appl. Phys., vol. 10, no. 2, pp. 565–569, 2010, doi: 10.1016/j.cap.2009.07.023.
[26] Z. Ghorannevis, M. T. Hosseinnejad, M. Habibi, and P. Golmahdi, Effect of substrate temperature on structural, morphological and optical properties of deposited Al/ZnO films, J. Theor. Appl. Phys., vol. 9, no. 1, pp. 33–38, 2015, doi: 10.1007/s40094-014-0157-1.
[27] S. Nagar, Disseratation: Multifunctional magnetic materials prepared by Pulsed Laser Deposition, 2012.
[28] H. Kim et al., Effect of film thickness on the properties of indium tin oxide thin films, J. Appl. Phys., vol. 88, no. 10, pp. 6021–6025, 2000, doi: 10.1063/1.1318368.
[29] M. Ben Rabeh, N. Khedmi, M. A. Fodha, and M. Kanzari, The effect of thickness on optical band gap and N-type conductivity of CuInS2 thin films annealed in air atmosphere, Energy Procedia, vol. 44, no. May 2013, pp. 52–60, 2014, doi: 10.1016/j.egypro.2013.12.009.
[30] H. Soonmin, A Brief Review of the Growth of Pulsed Laser Deposited Thin Films, Br. J. Appl. Sci. Technol., vol. 14, no. 6, pp. 1–6, 2016, doi: 10.9734/bjast/2016/22778.
[31] K. A. Aadim, N. K. Abbas, and A. T. Dahham, Influence the number of laser pulses and annealing temperature and the Structure and optical properties of In2O3: CdO films prepared laser induce plasma, Iraqi J. Sci., vol. 59, no. 3, pp. 1567–1576, 2018, doi: 10.24996/IJS.2018.59.3C.4.
[32] G. Balakrishnan, T. N. Sairam, V. R. Reddy, P. Kuppusami, and J. Il Song, Microstructure and optical properties of Al2O 3/ZrO2 nano multilayer thin films prepared by pulsed laser deposition, Mater. Chem. Phys., vol. 140, no. 1, pp. 60–65, 2013, doi: 10.1016/j.matchemphys.2013.02.053.